Dopamine transporters govern diurnal variation in extracellular dopamine tone

Mark J. Ferris[a], Rodrigo A. España[b], Jason L. Locke[a], Joanne K. Konstantopoulos[a], Jamie H. Rose[a], Rong Chen[a], and Sara R. Jones[a,1]

[a]Department of Physiology and Pharmacology, Wake Forest School of Medicine, Winston-Salem, NC 27157; and [b]Department of Neurobiology and Anatomy, Drexel University College of Medicine, Philadelphia, PA 19129

Edited by Richard D. Palmiter, University of Washington, Seattle, WA, and approved May 20, 2014 (received for review May 1, 2014)

The majority of neurotransmitter systems shows variations in state-dependent cell firing rates that are mechanistically linked to variations in extracellular levels, or tone, of their respective neurotransmitter. Diurnal variation in dopamine tone has also been demonstrated within the striatum, but this neurotransmitter is unique, in that variation in dopamine tone is likely not related to dopamine cell firing; this is largely because of the observation that midbrain dopamine neurons do not display diurnal fluctuations in firing rates. Therefore, we conducted a systematic investigation of possible mechanisms for the variation in extracellular dopamine tone. Using microdialysis and fast-scan cyclic voltammetry in rats, as well as wild-type and dopamine transporter (DAT) knock-out mice, we demonstrate that dopamine uptake through the DAT and the magnitude of subsecond dopamine release is inversely related to the magnitude of extracellular dopamine tone. We investigated dopamine metabolism, uptake, release, D2 autoreceptor sensitivity, and tyrosine hydroxylase expression and activity as mechanisms for this variation. Using this approach, we have pinpointed the DAT as a critical governor of diurnal variation in extracellular dopamine tone and, as a consequence, influencing the magnitude of electrically stimulated dopamine release. Understanding diurnal variation in dopamine tone is critical for understanding and treating the multitude of psychiatric disorders that originate from perturbations of the dopamine system.

circadian | caudate-putamen | nucleus accumbens

The dopamine transporter (DAT) is a transmembrane protein that removes dopamine (DA) from the extracellular space to terminate signaling at pre- and postsynaptic receptors. Extensive evidence indicates that aberrant DAT function may be involved in many neuropsychiatric illnesses, including attention deficit hyperactivity disorder (1, 2), depression (3, 4), substance abuse disorders (5, 6), schizophrenia (7–9), and anxiety disorders (10, 11). Our current understanding of the role of the DAT under physiologically normal conditions is that of a homeostatic regulator. This basic hypothesis was confirmed in work using DAT knock-out (KO) mice, where extracellular DA levels ($[DA]_{ext}$) and corresponding locomotor activity are substantially higher than in WT animals (12, 13). In addition, up- or down-regulation of the DAT is regarded as a compensatory plasticity to "normalize" $[DA]_{ext}$ in the context of repeated exposure to abused drugs (5, 14, 15).

Despite this progress in understanding DAT function, much less work has been dedicated to understanding the role of the DAT and other presynaptic modulators of $[DA]_{ext}$ over time periods that extend across the light and dark phases. Diurnal variations in $[DA]_{ext}$ have been demonstrated within the striatum (16–18), but are not related to variations in DA cell firing, because midbrain DA neurons do not display diurnal fluctuations in firing rates (19–23; but see ref. 24). This finding is in stark contrast to other neurotransmitter systems (e.g., serotonin, norepinephrine, and histamine), which show variation in state-dependent firing that is mechanistically linked to their respective extracellular levels or tone (25–30). Given the controversy surrounding the link between DA firing and $[DA]_{ext}$, we performed a systematic investigation of how variations in subsecond DA release and uptake relate to variations in $[DA]_{ext}$.

Despite the limited mechanistic understanding of the complex relationship between $[DA]_{ext}$ and nerve terminal function, behaviors known to be governed by DA are strongly influenced by diurnal cycles. For example, behaviors that measure reinforcement and reward, such as psychostimulant self-administration and conditioned place preference, fluctuate markedly across the light/dark cycle (31–34). Given that DA signaling is critical to the reinforcing and rewarding properties of drugs, it is possible that variations in DA signaling may drive the diurnal fluctuations observed in drug-associated behaviors. Therefore, the goal of the current project was to define diurnal variation in $[DA]_{ext}$ and to fully investigate the mechanisms that underlie such variation. We therefore measured $[DA]_{ext}$, extracellular DA metabolite levels, D2 autoreceptor sensitivity, tyrosine hydroxylase (TH) expression, TH activity, subsecond electrically stimulated DA release ($[DA]_o$), and DA uptake activity across the light/dark cycle and manipulated these parameters to understand their relationships and mechanistic links. We predicted that if the ability of DAT to recover $[DA]_{ext}$ was driving oscillations in $[DA]_{ext}$, then DA uptake by the DAT should be inversely related to $[DA]_{ext}$. In other words, DA uptake should be slowest when $[DA]_{ext}$ reaches peak levels, and fastest when $[DA]_{ext}$ reaches a trough.

Results

Diurnal Oscillations in Extracellular DA and Metabolites. First, we monitored extracellular DA and metabolite levels over 36 consecutive hours using microdialysis in awake, freely moving rats and recorded subsecond DA release and uptake kinetics using

Significance

The mechanism for diurnal (i.e., light/dark) oscillations in extracellular dopamine tone in mesolimbic and nigrostriatal systems is unknown. This is because, unlike other neurotransmitter systems, variation in dopamine tone does not correlate with variation in dopamine cell firing. The current research pinpoints the dopamine transporter as a critical governor of diurnal variation in both extracellular dopamine tone and the intracellular availability of releasable dopamine. These data describe shifts in the function of the dopamine system over time, which may have implications for diurnal effects on dopamine-dependent learning, sleep/wake behavior, locomotor activity, reward, and drug addiction.

Author contributions: M.J.F., R.A.E., and S.R.J. designed research; M.J.F., J.L.L., J.K.K., and J.H.R. performed research; R.C. and S.R.J. contributed new reagents/analytic tools; M.J.F. analyzed data; and M.J.F. and R.A.E. wrote the paper.

The authors declare no conflict of interest.

This article is a PNAS Direct Submission.

[1]To whom correspondence should be addressed. E-mail: srjones@wakehealth.edu.

This article contains supporting information online at www.pnas.org/lookup/suppl/doi:10.1073/pnas.1407935111/-/DCSupplemental.

fast-scan cyclic voltammetry (FSCV) in brain slices of rats at 6-h intervals on a 12-h light/dark cycle. Fig. 1*A* demonstrates that $[DA]_{ext}$ oscillates in a sinusoidal fashion (third-order best-fit model) that is significantly different from linearity [$F_{(2,291)}$ = 28.9, $P < 0.0001$], with the peak and trough occurring midway through the dark and light phases, respectively. The DA metabolites, homovanillic acid (HVA) (Fig. 1*B*) , and 3,4-dihydroxyphenylacetic acid (DOPAC) (Fig. 1*C*), also oscillated according to a third-order model that significantly deviated from linearity ($P < 0.0001$) with the primary DA metabolite (DOPAC) offset in time from DA by 6 h (Fig. 1*D*), consistent with the well-documented slow time course of metabolism.

The Rate of DA Uptake Is Inversely Related to Extracellular DA Levels. Given the notion that the DAT is a homeostatic regulator of $[DA]_{ext}$, we investigated whether there was diurnal variation in DA uptake across four strategically selected, equally spaced time points [zeitgeber time (ZT)1, ZT6, ZT13, ZT18] across the light/dark cycle using voltammetry in rat brain slices. Maximal rates of DA uptake (V_{max}) demonstrated a significant inverted U-shaped trend in the caudate-putamen (CPu) (Fig. 2*A*), nucleus accumbens (NAc) core (Fig. 2*B*), and NAc shell (Fig. 2*C*) when plotted across time, starting at ZT1. Fig. 2*D* describes an inverse relationship between V_{max} and $[DA]_{ext}$, such that the fastest V_{max} (ZT6) occurred when $[DA]_{ext}$ was at the lowest levels, whereas the slowest V_{max} (ZT18) occurred when $[DA]_{ext}$ was at the highest levels. Tukey's multiple comparison post hoc test indicated the most robust differences midway through the light (ZT6) and dark (ZT18) phases (Fig. 2 *A*–*C*). Furthermore, linear regression of the slopes between ZT18 and ZT6 in Fig. S1 showed an increase in V_{max} at a rate of 8.78% per hour with a corresponding decrease in $[DA]_{ext}$ of 2.6% per hour.

The Magnitude of Rapid DA Release Is Inversely Related to Extracellular DA Levels. We next measured diurnal variation in the peak-height of electrically stimulated DA transients ($[DA]_o$) across the same four time points measured for uptake data using voltammetry in rat brain slices. Similar to V_{max}, single-pulse stimulations produced a significant quadratic, inverted U-shaped trend in $[DA]_o$ when plotting across time, starting 1 h into the light phase (ZT1). This trend was evident in CPu (Fig. 3*A*), NAc core (Fig. 3*B*), and NAc shell (Fig. 3*C*). Additionally, there was a main effect of time-of-day for each region (CPu and core, $P < 0.001$; shell, $P < 0.01$), with Tukey's multiple comparison post hoc test indicating the most robust differences midway through the light (ZT6) and dark (ZT18) phases (Fig. 3 *A*–*C*). Fig. 3*D* shows the predicted inverse relationship between stimulated $[DA]_o$ and $[DA]_{ext}$ when both are normalized and plotted in the same graph. Indeed, the amount of stimulated $[DA]_o$ is lowest midway through the dark phase, a time that is characterized by highest $[DA]_{ext}$. The inverse relationship is exhibited in the light phase such that when stimulated $[DA]_o$ is highest, $[DA]_{ext}$ is at the lowest point. This relationship is consistent with the idea that $[DA]_{ext}$ is recycled back into DA nerve terminals via an uptake mechanism and is packaged into vesicles for release (35, 36), with the efficiency of V_{max} determining the magnitude of $[DA]_o$.

D2 Autoreceptor Sensitivity Is Synchronous with Extracellular DA Levels. Oscillations in the sensitivity of D2 autoreceptors could contribute to changes in $[DA]_{ext}$. The ability of D2 autoreceptors to inhibit $[DA]_o$ was measured using the D2-agonist, quinpirole, using voltammetry in rat brain slices. Investigating $[DA]_o$ elicited by single-pulse stimulations in a brain slice preparation allows for interrogation of presynaptic D2 autoreceptors because quinpirole does not modulate $[DA]_o$ in mice with genetic knock-out of presynaptic D2 autoreceptors (37). Therefore, there is little to no documented effect of quinpirole modulating $[DA]_o$ via postsynaptic D2 signaling when using slice voltammetry (37). There were significant changes in the ability of the quinpirole to reduce $[DA]_o$ across the light/dark cycle. Fig. 4 *A* and *B* show that quinpirole (30 nM and 100 nM, respectively) reduced electrically stimulated DA release to a greater extent in the dark phase, with the most robust effects occurring midway through the dark phase (ZT18). Next, data from Fig. 4*A* were expressed as a percent of

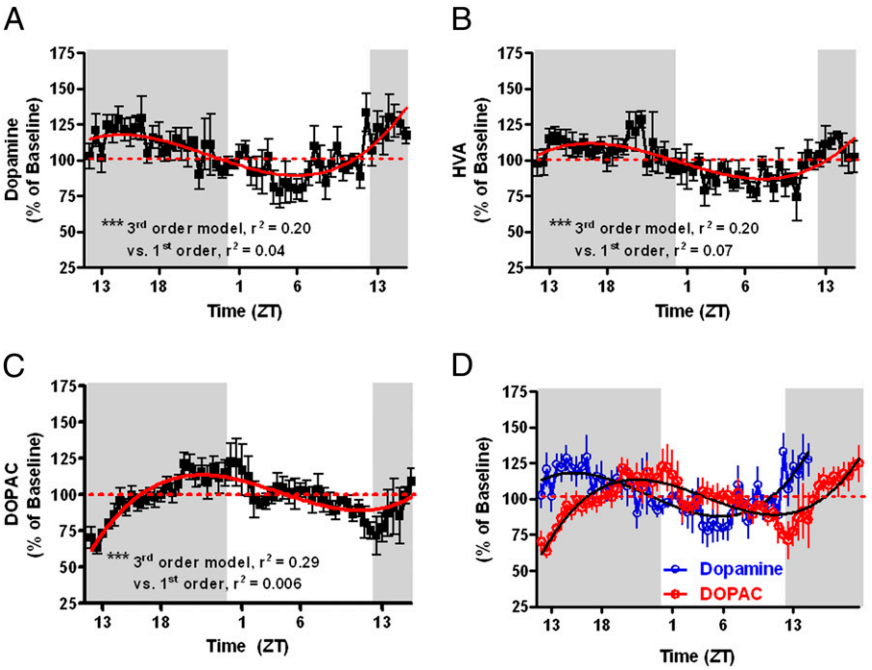

Fig. 1. Extracellular dopamine (*A*) and metabolites HVA (*B*) and DOPAC (*C*), expressed as percent of baseline, oscillate across the light/dark cycle with peaks and trough of DA and HVA occurring midway through the dark and light phases, respectively. The DOPAC cycle is phase-shifted to the right of dopamine by ~6 h (*D*). DA, HVA, and DOPAC are best fit to a third-order regression curve that is significantly different from linearity (***$P < 0.001$).

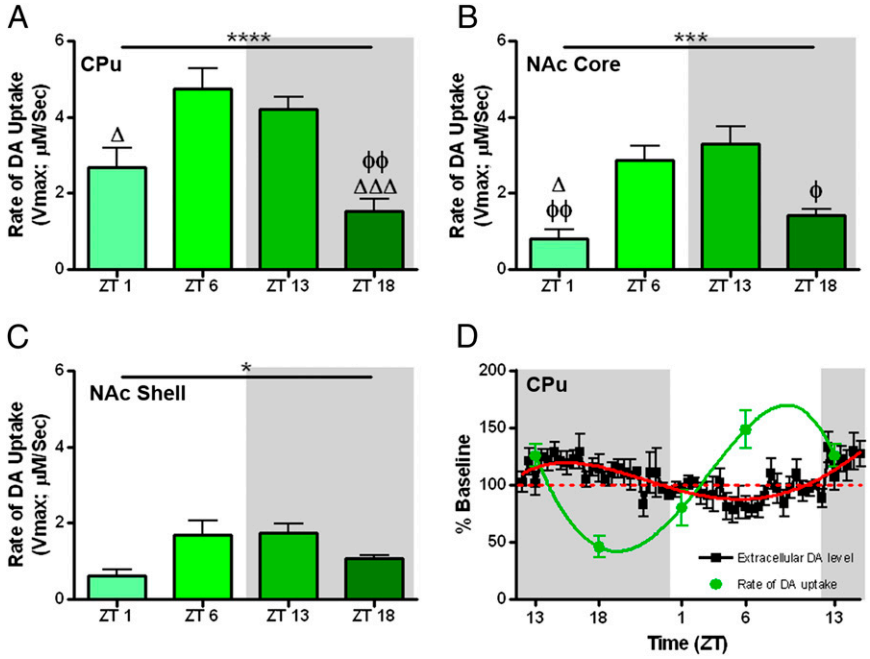

Fig. 2. Maximal rate of DA uptake (V_{max}) in the caudate (*A*), NAc core (*B*), and shell (*C*) engenders an inverted u-shaped trend when plotted starting one hour into the light phase (ZT1; main effect of ZT, $^{***}P < 0.001$, $^{**}P < 0.01$). Tukey's multiple comparisons ($^{\Delta\Delta\Delta}P < 0.001$, $^{\Delta}P < 0.05$ relative to ZT6; $^{\Phi\Phi}P < 0.01$, $^{\Phi}P < 0.05$ relative to ZT13). V_{max} demonstrates an inverse relationship to extracellular dopamine levels ($[DA]_{ext}$) in the caudate (*D*). The green line represents the best-fit model for V_{max} and the red line represents the best-fit model for $[DA]_{ext}$.

the mean effect of quinpirole across the four time points, then inverted and plotted against $[DA]_{ext}$ in Fig. 4*C* to evaluate the relative sensitivity of autoreceptors relative to $[DA]_{ext}$. Thus, greater inhibition of $[DA]_o$ by quinpirole, when inverted, translates to greater sensitivity of D2 autoreceptors in Fig. 4*C*. The sensitivity of D2 autoreceptors oscillates in a manner almost identical to $[DA]_{ext}$. Specifically, autoreceptors are at their greatest sensitivity during the dark phase when $[DA]_{ext}$ is highest, and are the least sensitive during the light phase when $[DA]_{ext}$ is lowest. This synchrony suggests two points. The first point is that the sensitivity of D2-autoreceptors does not drive $[DA]_{ext}$ directly, as one would expect high $[DA]_{ext}$ when D2 autoreceptors are less able to inhibit DA release for this to be the case. The second point is that $[DA]_{ext}$ does not drive D2R sensitivity, as the extant literature would predict low D2R sensitivity when $[DA]_{ext}$ is high. Indeed, G protein-coupled receptors are thought to desensitize as they are activated by their endogenous ligands. It is possible that $[DA]_{ext}$ does not reach levels high or low enough across the light/dark cycle to affect receptor sensitivity.

The DA Transporter Is Necessary for Diurnal Variation in Extracellular DA Levels. Ruling out D2 autoreceptors provides additional evidence that DAT function drives oscillations in $[DA]_{ext}$. Furthermore, the ability of the DAT to take up DA appears to control levels of intracellular, releasable DA. To fully test the hypothesis that V_{max} is the mechanism that drives $[DA]_{ext}$, we monitored $[DA]_{ext}$ for 36 consecutive hours using microdialysis in awake, freely moving mice with and without a genetic knock out of DAT (DAT KO and WT, respectively). Additionally, we recorded release and uptake kinetics using FSCV in brain slices from WT and KO mice. As was the case for rat $[DA]_{ext}$, Fig. 5*A* demonstrates that $[DA]_{ext}$ in WT mice oscillates in a sinusoidal fashion (fourth-order best fit) that is significantly different from linearity [$F_{(3,314)} = 65.4$, $P < 0.0001$], with the peak and trough occurring midway through the dark and light phases, respectively. Contrary to WT mice, DAT KO mice demonstrated no sinusoidal oscillation in $[DA]_{ext}$, which was best fit by a straight line model (first order) with no slope ($\beta = 0.044$) (Fig. 5*B*). Both third- and fourth-order models, which would be indicative of sinusoidal oscillation, would not fit when forced on the data ($R^2 = 0.0001$, $P = 0.98$). The lack of diurnal oscillation of $[DA]_{ext}$ in DAT KO mice indicates that the DAT is necessary for diurnal oscillations in $[DA]_{ext}$. These findings, combined with the inverse relationship between $[DA]_{ext}$ and the rate of DA uptake, leads to the conclusion that diurnal oscillations in the function of the DAT drive oscillations in $[DA]_{ext}$.

Oscillations in the Level and Activity of TH Cannot Account for Diurnal Variation in Extracellular DA Levels. Oscillations in the level or activity of TH could contribute to changes in $[DA]_{ext}$ independent of oscillations in DA uptake. Therefore, we examined both the levels and activity of TH across the four time points in the light/dark cycle in both WT and DAT KO mice. Similar to previously published reports (38, 39), Western blot analysis revealed that TH levels oscillated in a manner similar to $[DA]_{ext}$ in WT mice. Indeed, Fig. 5*C* (green) shows TH expression in WT mice oscillated in a sinusoidal fashion, with the peak and trough occurring midway through the dark and light phases, respectively. Consistent with TH levels, we show that the activity of TH, as measured by L-dopa (L-DOPA) accumulation after DOPA decarboxylase inhibition with systemic injection of NSD-1015 (Fig. 5*C*, blue symbols), oscillated in a manner almost identical to both $[DA]_{ext}$ and TH levels in WT mice (Fig. 5*C*, blue). Namely, L-DOPA in WT mice oscillated in a sinusoidal fashion (third-order best fit) that was significantly different from linearity [$F_{(2,22)} = 5.70$, $P < 0.01$], with the peak and trough occurring midway through the dark and light phases, respectively.

We next measured TH levels and activity across the four time points in the DAT KO mice that, as shown above, do not express diurnal oscillations in $[DA]_{ext}$. Western blot analysis of TH protein levels in the striatum revealed that despite no variation in $[DA]_{ext}$, TH levels in DAT KO mice oscillated in a manner almost identical to WT mice (Fig. 5*D*). The sinusoidal curve (third-order best fit) was significantly different from linearity

[$F_{(2,23)}$ = 6.78, $P < 0.05$], with the peak and trough occurring midway through the dark and light phases, respectively. There was no significant difference in TH levels between WT and DAT KO mice when expressed as a percent baseline (i.e., compare green points in Fig. 5 *C* and *D*). The nonsignificant trend toward lower-magnitude shifts in WT TH levels relative to DAT KO animals occurred because, consistent with previous literature (40), we observed significantly higher absolute TH protein levels in WT mice (mean ± SEM = 1.27 ± 0.07) relative to DAT KO mice [mean ± SEM = 0.89 ± 0.07, $t_{(41)}$ = 3.72, $P < 0.001$]. Because shifts in absolute TH levels are of similar magnitude in both strains ($P > 0.05$), the higher baseline levels in WT mice appear to attenuate shifts in this strain when they are expressed as percent of baseline levels.

L-DOPA levels oscillated in DAT KO mice, with the peak and trough occurring midway through the dark and light phases, respectively. This finding was almost identical to TH activity in WT and DAT KO mice, and in a manner consistent with L-DOPA levels in WT mice. Therefore, both TH levels and activity (as measured by L-DOPA accumulation) oscillate in DAT KO and WT mice in a similar, diurnal fashion. This similarity is compelling evidence that DA synthesis, as measured by TH protein levels and activity, cannot solely contribute to, and is not sufficient for, diurnal variation in $[DA]_{ext}$. Similar to TH levels described above, there was no significant difference in L-DOPA levels between WT and DAT KO mice when expressed as a percent baseline (i.e., compare blue points in Fig. 5 *C* and *D*). The nonsignificant trend toward lower magnitude shifts in DAT KO levels of L-DOPA relative to WT animals occurred because, consistent with previous literature (40), we observed significantly higher absolute L-DOPA levels in DAT KO mice (mean ± SEM = 202.8 ng/mg ± 15.52) relative to WT mice [mean ± SEM = 135.1 ng/mg ± 9.96, $t_{(40)}$ = 3.67, $P < 0.001$]. Because shifts in absolute L-DOPA are of similar magnitude in both strains ($P > 0.05$), the higher baseline levels in DAT KO mice appear to attenuate shifts in this strain when they are expressed as percent of baseline levels.

The DAT Is Necessary for Diurnal Variation in the Magnitude of Rapid DA Release. If variation in $[DA]_{ext}$ at the time of slice preparation determines variation in $[DA]_o$, as suggested by our rat voltammetry data (Fig. 2*D*), then we would predict that DAT KO mice would show no variation in $[DA]_o$ across the light/dark cycle. To this end, we killed WT and DAT KO mice at two time points (midway through dark, ZT18; and midway through light, ZT6), which correspond to the peak and trough of $[DA]_{ext}$ in WT animals, and measured $[DA]_o$ using voltammetry in brain slices. As predicted, Fig. 6 (green bars) shows that $[DA]_o$ in WT mice was identical to the rat data where $[DA]_o$ was significantly greater midway through the light phase (ZT6) than midway through the dark phase (ZT18) [$t_{(13)}$ = 3.31, $P < 0.01$]. Unlike WT mice and rats, DAT KO mice exhibited no change in $[DA]_o$ (Fig. 6, blue bars), which is consistent with the lack of variation in $[DA]_{ext}$ across the light/dark cycle. Given these data, we predicted that oscillations in $[DA]_{ext}$ that occur over the course of many hours before killing a WT animal ultimately determine oscillations in $[DA]_o$ in the slice preparation. This explanation is based on the notion that the rate of DA uptake can bias DA levels to an intracellular or extracellular location over many hours. Indeed, the DAT has been directly linked to the recycling of DA and the filling of readily releasable vesicles (35, 36). We argue that this occurs over time and to an increasing extent leading up to midway through light phase. This is a time when the rate of DA uptake through the DAT is high, allowing for more efficient filling of vesicles. This mechanism would lead to greater readily releasable $[DA]_o$ when DA is biased to an intracellular location in the light relative to the dark. To test this hypothesis, we implanted WT mice with osmotic minipumps that delivered cocaine (7.5 mg·kg·h) for 48 consecutive hours to block DA uptake for two complete diurnal cycles before sacrifice. In a manner similar to the DAT KO mice, WT mice outfitted with

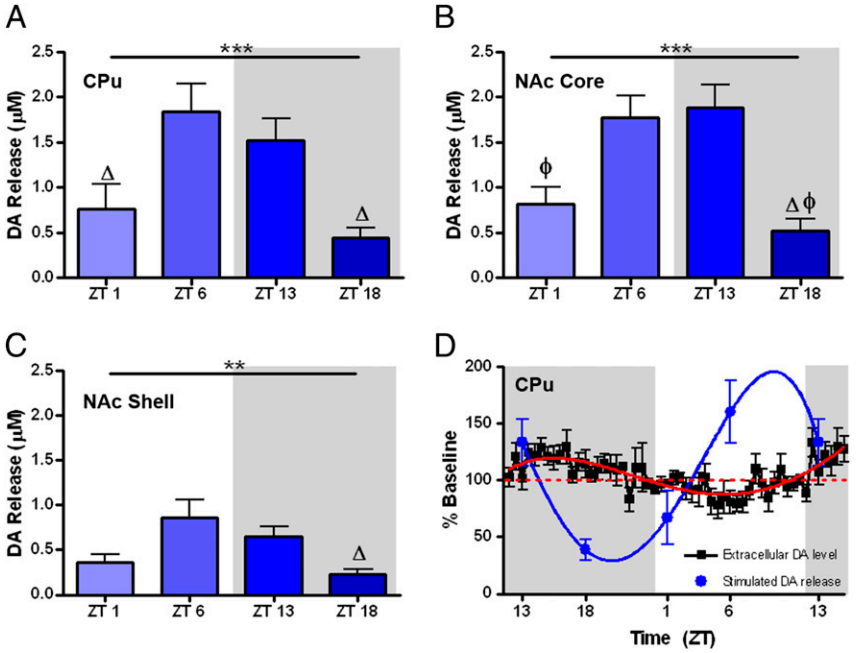

Fig. 3. Electrically-stimulated dopamine release ($[DA]_o$) in the caudate (*A*), NAc core (*B*), and shell (*C*) engenders an inverted u-shaped trend when plotted starting 1 h into the light phase (ZT1; main effect of ZT, $***P < 0.001$, $**P < 0.01$). Tukey's multiple comparisons ($^{\Delta}P < 0.05$ relative to ZT6; $^{\Phi}P < 0.05$ relative to ZT13). (*D*) $[DA]_o$ demonstrates an inverse relationship to extracellular dopamine levels ($[DA]_{ext}$) in the caudate. The blue line represents the best-fit model for $[DA]_o$ and the red line represents the best-fit model for $[DA]_{ext}$.

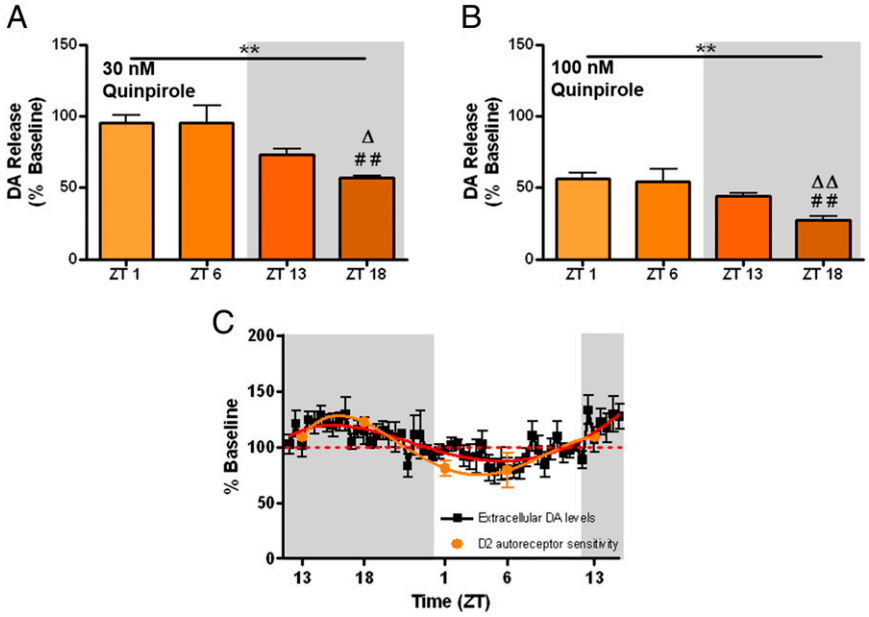

Fig. 4. Electrically stimulated DA release ($[DA]_o$) in the caudate following 30 nM (*A*) and 100 nM (*B*) quinpirole, expressed as a percent of predrug $[DA]_o$ engenders a decreasing linear trend when plotted starting one hour into the light phase (ZT1; main effect of ZT, $^{**}P < 0.01$). Tukey's multiple comparisons ($^{\#\#}P < 0.01$ relative to ZT1; $^{\Delta\Delta}P < 0.01$, $^{\Delta}P < 0.05$ relative to ZT6). (*C*) The relative sensitivity of caudate D2 autoreceptors to inhibit $[DA]_o$ is plotted against extracellular DA in the caudate.

cocaine minipumps exhibited no change in $[DA]_o$ between ZT6 and ZT18 (Fig. 6, orange bars). These results are consistent with DAT function being required for diurnal cycling of DA, as well as DA being recycled by an uptake mechanism and therefore biased toward an intracellular location and ready for release upon electrical stimulation when the rate of DA uptake is high.

To confirm that many hours of attenuated recycling and accumulation of intracellular DA through reduced DAT function were required to decrease $[DA]_o$, we added an acute, high dose of cocaine (10 μM) to the bath of brain slices from WT mice to block DA uptake after slice preparation. Because there is no $[DA]_{ext}$ in a slice preparation, the amount of readily releasable $[DA]_o$ should be limited to intracellular DA levels that were present at the time of sacrifice. Despite the acute pharmacological blockade of DAT, differences between ZT6 and ZT18 remain in this group (Fig. 6, red bars) [$t_{(10)} = 2.30$, $P < 0.05$]. Therefore, acute pharmacological blockade of DAT in slices from WT mice is not sufficient for reconciling the difference between light and dark phases, and does not recapitulate data observed in DAT KO mice or mice with cocaine minipumps. This finding rules out the contribution of acute blockade of DAT in a slice to modulate variation in diurnal $[DA]_o$. Moreover, $[DA]_o$ is significantly enhanced at ZT6 and not at ZT18 following acute cocaine application (Fig. 6, green vs. red bars) [$t_{(16)} = 1.88$, $P < 0.05$]. The fact that $[DA]_o$ can be augmented by DA uptake inhibition at this time point suggests that more DA is available for release at a time when there are augmented levels of intracellular, readily releasable DA.

Discussion

The activity of DA neurons does not fluctuate across the light/dark cycle (19–23), so it is possible that variations in $[DA]_{ext}$ are associated with variation in the ability of the DAT to take up DA into the nerve terminals and effectively offset release (i.e., maintain homeostasis). Diurnal variation in the density of cell-surface DAT (38, 39) and some changes in DA uptake kinetics have been noted (41, 42); however, no work has systematically compared variations in DA uptake to the number of parameters investigated herein. Therefore, our initial experiments focused on examining the extent to which uptake fluctuated across the light/dark cycle. We demonstrate that DA uptake through the DAT and the magnitude of evoked, subsecond $[DA]_o$ is inversely related to the magnitude of $[DA]_{ext}$, with fastest uptake occurring when $[DA]_{ext}$ is lowest, and slowest uptake occurring when $[DA]_{ext}$ peaks.

Neither metabolism nor autoreceptor inhibition of DA can account for the diurnal variation in $[DA]_{ext}$. The metabolites HVA and DOPAC were either time-locked to DA rhythms or delayed for as much as 6 h, respectively. This finding replicates earlier work (43) and strongly suggests that although metabolism actively degrades DA, it is not a mechanism for variations in $[DA]_{ext}$. Rather, metabolite levels oscillate as a function of the variation in $[DA]_{ext}$. Similar to metabolites, D2 autoreceptor sensitivity varies synchronously with $[DA]_{ext}$, such that highly sensitive D2R are associated with high $[DA]_{ext}$. This relationship is the opposite of what would be expected if D2R governed $[DA]_{ext}$ or vice-versa, suggesting no immediately interpretable causal link between the two. To our knowledge, research investigating oscillations in D2R function across the light/dark cycle have not segregated pre- and postsynaptic D2R populations, with interpretations usually favoring implications from a postsynaptic perspective. However, $[DA]_o$ elicited by single pulse stimulations in brain slices is considered too rapid to be influenced by retrograde signaling that would be mediated by postsynaptic D2 receptors. Furthermore, Bello et al. (37) demonstrated that the contribution of quinpirole on postsynaptic D2R to modulate $[DA]_o$ as measure by voltammetry in brain slices is negligible compared with the direct inhibitory influence of quinpirole on D2 autoreceptors. Therefore, to our knowledge, this is the first specific demonstration of diurnal oscillations in presynaptic D2 autoreceptor function. Although light/dark differences in D2R function vary across studies, increased sensitivity of D2R during the dark phase is congruent with work in mice demonstrating substantially higher [^{125}I]sulpiride binding in the striatum during the dark phase (38), larger responses to apomorphine during the dark phase in rats (44), and larger reflexive

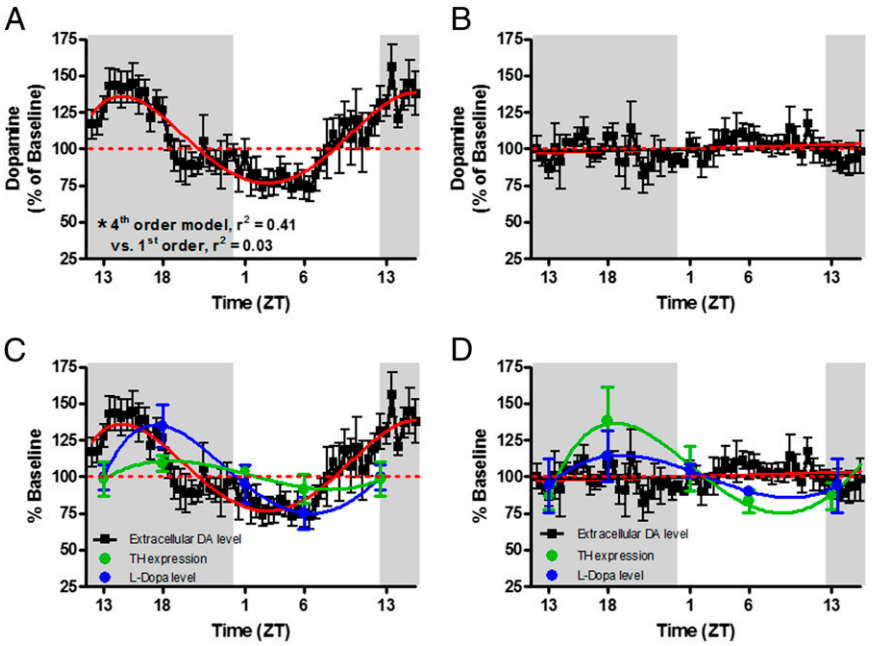

Fig. 5. Extracellular dopamine $[DA]_{ext}$ in the caudate of WT mice (*A*) oscillates across the light/dark cycle. The red line signifies a fourth-order regression best-fit model that was significantly different from linearity (***$P < 0.001$). DAT KO mice (*B*), demonstrated no light/dark cycle oscillation in $[DA]_{ext}$. TH expression (green line) and activity (blue line; as measured by L-DOPA accumulation after administration of NSD-1015) oscillates in both WT (*C*) and DAT KO (*D*) mice in a manner similar to $[DA]_{ext}$ in WT mice.

locomotor responses to quinpirole during the dark in *Drosophila melanogaster* (45).

In contrast to metabolism and D2 autoreceptor activity, we show with a number of experiments that variation in the efficiency of DA uptake governs $[DA]_{ext}$. First, we demonstrated that more rapid uptake of DA occurs during the light phase when $[DA]_{ext}$ is low, and a slowing of DA uptake occurs during the dark phase when $[DA]_{ext}$ is high. Indeed, this result is congruent with research showing increased cell-surface DAT during the light phase (38); this placed the efficiency of DA uptake in an ideal position to be mechanistically linked to $[DA]_{ext}$. Furthermore, blockade of DAT with genetic modification or pharmacological intervention leads to elevated $[DA]_{ext}$, so it is perfectly reasonable that physiological variation in the efficiency of DAT would lead to variation in $[DA]_{ext}$. In fact, recent mathematical models highlight transporter concentration (i.e., cell-surface expression) as a critical component of neurotransmitter homeostasis (46). Second, we confirmed the necessity of DAT in mediating diurnal variation in $[DA]_{ext}$ by documenting a lack of variation in $[DA]_{ext}$ in DAT KO mice. Third, we showed that diurnal variations in TH levels and activity are present not only in WT mice, as shown previously (38, 39), but also in DAT KO mice that show no variation in $[DA]_{ext}$. TH is therefore not sufficient for mediating diurnal variations in $[DA]_{ext}$ because $[DA]_{ext}$ cannot vary without the DAT, despite oscillations in TH expression and activity.

Based on this evidence, we propose a model for the diurnal regulation of $[DA]_{ext}$, whereby lower rates of DA uptake midway through the dark phase (likely via decreased cell surface DAT expression) lead to a predominantly extracellular location of DA, whereas faster rates of DA uptake midway through the light phase (likely via increased cell surface DAT expression) lead to a predominantly intracellular location of DA. Indeed, the DAT has been explicitly linked to the recycling of $[DA]_{ext}$ and the filling of readily releasable vesicles (35, 36). This DAT-driven intracellular vs. extracellular location of DA is confirmed by our demonstration of the oscillation in magnitude of subsecond $[DA]_o$ upon stimulation. Intracellular availability of DA in vesicles is a limiting factor in the magnitude of $[DA]_o$ in voltammetry experiments (40), suggesting lower intracellular availability when $[DA]_{ext}$ is high. Notably, we prevented the diurnal variation in $[DA]_o$ in mice where the DAT is genetically inactivated. DAT KO mice exhibit extremely high, fivefold increase in $[DA]_{ext}$ (40), and a 95% depletion of intracellular DA, suggesting uptake is necessary for intracellular storage of DA. Furthermore, in DAT KO mice vesicular DA levels were the limiting factor in the magnitude of $[DA]_o$ (40), suggesting lower intracellular availability of DA when DAT is fewer. Note that acute blockade of DA uptake directly on a slice with a saturating concentration of cocaine failed to reconcile diurnal differences in $[DA]_o$. This finding is fully consistent with our model and may be attributed to the fact that acute blockade of the DAT in these experiments occurred after DA had already shifted to a predominantly intra- vs. extracellular location. We propose that this shift occurs over the course of several hours across the light/dark cycle, and therefore can only be blocked in experiments with sustained DAT blockade. Specifically, we showed that pharmacological blockade of DA uptake with continuous exposure to cocaine for 48 h in vivo, via minipumps, mimicked the effects demonstrated in DAT KO mice. These experiments suggest that the DAT is necessary for the movement of DA from predominantly intra- vs. extracellular locations. Namely, intracellular DA that is available for stimulated release may be low when uptake rates are slow enough to "bias" DA toward a primarily extracellular location, and $[DA]_o$ may be high when uptake rates are rapid enough to supply high intracellular DA levels. Although the DAT influences $[DA]_o$ over time as described here, it is apparent that other mechanisms must also be influencing $[DA]_o$ given that the magnitude of the observed shift in $[DA]_{ext}$ cannot solely account for the relatively larger shift in $[DA]_o$ magnitude. Therefore, it is also important to consider other mechanisms that are known to regulate the probability of release and may play a role in diurnal regulation of DA release magnitude. For example, Cragg et al. (47, 48) have shown that the probability and magnitude of release elicited by electrical

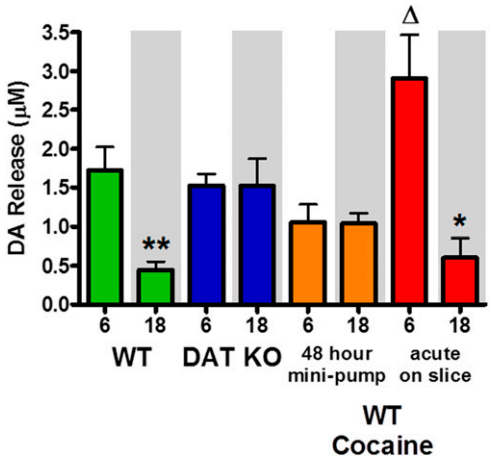

Fig. 6. Stimulated dopamine release $[DA]_o$ is higher during the light in WT (green, $^{**}P < 0.01$), but not DAT KO (blue) mice. Cocaine eliminated variation in $[DA]_o$ when administered for 48 consecutive hours in vivo via mini-pump (orange bars) but augmented the difference in $[DA]_o$ between the light and dark in WT mice when applied acutely to brain slices ($^{**}P < 0.01$, $^{*}P < 0.05$; $^{\Delta}P < 0.05$ red vs. green ZT6).

stimulation varies across subregions of the striatum, and depends on the amount of available calcium (47) and tissue content of DA (48). Thus, it is possible that calcium levels, among other factors, are diurnally regulated and impact the probability and magnitude of $[DA]_o$.

Regardless of the specific mechanisms, diurnal variation in the magnitude of $[DA]_o$ suggests that there may be diurnal changes in postsynaptic receptor activation resulting from phasic DA release. The D1 receptor is thought to be activated by higher-amplitude, phasic release events because of their relative low affinity for DA, whereas the D2 receptors have higher affinity for DA and are activated by tonic $[DA]_{ext}$ (49). The relative balance of D1 and D2 receptor activation might lean toward less D1/more D2 activation during a time-of-day when $[DA]_{ext}$ is high and $[DA]_o$ is low (e.g., midway through dark phase), whereas the inverse might be true during a time-of-day when the balance shifts toward more $[DA]_o$ and less $[DA]_{ext}$ (e.g., midway through light phase). Nevertheless, the shifts in $[DA]_{ext}$ are relatively modest compared with shifts in $[DA]_o$, so the extent to which D2 receptor activation might be influenced by shifts in $[DA]_{ext}$ may be less than for shifts in $[DA]_o$ influencing D1 receptors.

Our results are consistent with research relating DAT levels/density and function to arousal. For example, decreased DAT density is associated with shorter sleep duration in humans (50) and lower DAT function is associated with increased arousal/wakefulness and decreased rest in fruit flies with mutations of the gene that encodes for DAT (51), in DAT KO mice (52), and in rhesus monkeys with chronic DAT inhibition (53). These data match our results indicating lower DA uptake via the DAT midway through the active/dark cycle, although caution should be taken in inferring changes in wakefulness from the relatively small diurnal fluctuation in DA compared with the large shifts observed in DAT KO mice and in rhesus monkeys with chronic DAT inhibition shown in previous work (52, 53). Thus, the DAT is a pharmacotherapeutic target for promoting wakefulness (54), and likely plays a critical role in clinical manifestations of some disorders that disturb both nighttime rest and daytime activity. For example, with respect to nighttime rest, recent work has shown decreased DAT levels (55) and increased DA (56) in patients with restless legs syndrome when assessed using real time imaging of the DAT. With respect to disruption of daytime activity, pharmacotherapeutic targets of the DAT (e.g., modafinil and amphetamine) are efficacious in the treatment of excessive daytime sleep disorders (52, 57–59). Therefore, the DAT likely plays a role in both ends of the sleep disorder spectrum, which is consistent with an uptake mechanism governing $[DA]_{ext}$. Additionally, it will be important to investigate altered cycling within a phase in addition to experiments aimed at understanding differences in the dark and light phases. For example, the frequency of periodic limb movements associated with restless legs syndrome changes within a single phase, and is more prominent during the early portion of the sleep period (60), which coincides with a time when our data demonstrate low uptake (ZT1).

In addition to implications for sleep regulation, these data also highlight the need for a paradigm shift within neuropharmacology from the idea that mesolimbic DA is a static system, whereby transporters and receptors simply up- or down-regulate following drug exposure, to the concept that it is a dynamic system that may become increasingly off-balance with drug experience and abuse. For example, it is noteworthy that 48 h of continuous cocaine exposure eliminated natural variation in $[DA]_o$. Although modern animal models of drug abuse typically limit drug intake, early studies show that animals given unlimited access to a drug will elect to administer psychostimulants continuously for days until crashing into bouts of sleep (61). Thus, it appears that under behaviorally plausible conditions of psychostimulant intake, cocaine disrupts diurnal variation in DA signaling. However, more research is needed to outline disruption of neurotransmitter signaling under conditions of more regulated drug intake.

In conclusion, we have pinpointed the DAT as a critical governor of diurnal variation in $[DA]_{ext}$ and an important regulator in the amount of releasable $[DA]_o$ over time. Future research should investigate whether these amplified DA signals may explain, at least in part, increased psychostimulant drug seeking during the active phase (34). These data outline underlying tenets of the basic physiology of the DA system over time, and likely have implications for DA-dependent learning, sleep/wake behavior, locomotor activity, reward, and drug addiction.

Methods

Subjects. Male Sprague–Dawley rats (375–400 g; Harlan Laboratories) and mice with and without genetic deletion of the DAT (28–35 g) were used as subjects. All animals were maintained on a 12-h light/dark cycle with food and water available ad libitum. Rats were double-housed and mice were housed in groups of three to five up until the time of surgery at which time they were singly-housed. All animals were maintained according to the National Institutes of Health (NIH) guidelines in Association for Assessment and Accreditation of Laboratory Animal Care-accredited facilities. The experimental protocol was approved by the Institutional Animal Care and Use Committee at Wake Forest School of Medicine.

Microdialysis. Microdialysis guide cannulae (CMA/Microdialysis) were stereotaxically implanted above the dorsal striatum (CPu) at coordinates anteroposterior +0.7 mm, lateral ±3.2 mm, ventral −3.0 mm for rat experiments, and coordinates anteroposterior +0.7 mm, lateral ±1.75 mm, ventral −2.5 mm for mouse experiments relative to bregma, midline, and skull surface (rat)/dura (mouse), respectively. Rats and mice recovered for 3–5 d after surgery before the start of experimentation. Concentric microdialysis probes (2 mm membrane length; CMA/Microdialysis) were inserted ~8 h before the beginning of sample collection and continuously perfused at 0.8 μL/min with artificial cerebrospinal fluid (aCSF) (pH 7.4) containing: NaCl (148 mM), KCl (2.7 mM), $CaCl_2$ (1.2 mM), $MgCl_2$ (0.85 mM). The outlet line of the microdialysis probe was connected directly to an HPLC injection loop, which would automatically inject sample once every 30 min. DA, DOPAC, and HVA levels were monitored online for 38 consecutive hours (two samples per hour) beginning at lights off.

HPLC and Tissue Content. All microdialysates were analyzed online by HPLC coupled to electrochemical detection at +220 mV (ESA Inc.). Neurotransmitters and their metabolites were separated on a Luna 100 × 3.0 mm C_{18} 3 μm

HPLC column (Phenomenex). The mobile phase consisted of 50 mM citric acid, 90 mM sodium dihydrogen phosphate, 1.7–2.0 mM 1-octanesulfonic acid, 50 μM ethylenediaminetetracetic acid, 10–12% (vol/vol) acetonitrile, and 0.3% triethylamine in a volume of 1 L (pH 3.0). Analytes were quantified using PowerChrom software (eDAQ) by comparison with a three point external standard curve bounding the expected range of analyte values.

For the tissue content/TH activity studies, DAT WT and DAT KO mice were killed at 1 and 6 h into the light and dark phases of the light/dark cycle, 40 min after pretreatment with 100 mg/kg 3-hydroxybenzylhydrazine dihydrochloride (NSD-1015; Sigma-Aldrich). NSD-1015 blocks the activity of DOPA decarboxlyase to prevent the transformation of L-DOPA into DA. This magnitude of L-DOPA accumulation under these conditions is a reliable measure of TH activity. The striatum was dissected, snap-frozen, and samples (10–30 mg per sample wet weight) were homogenized in 250 μL of 0.1 M $HClO_4$ and analyzed for protein concentration by the BCA method (Thermo Scientific). Extracts were centrifuged and the supernatants removed and analyzed for L-DOPA using HPLCy (HPLC) coupled to electrochemical detection at +220 mV (ESA Inc.) and separated on a Luna 100 × 3.0 mm C_{18} 3 μm HPLC column (Phenomenex). The mobile phase consisted of 5.99 g sodium dihydrogen phosphate, 200 μM EDTA, 0.584 g sodium chloride, 40 mg Octyl sulfate sodium salt, 100 mL Methanol, 1 L ultrapure water (pH 2.6). Analytes were quantified using PowerChrom software (eDAQ) and a calibration.

Fast-Scan Cyclic Voltammetry. For slice voltammetry experiments, animals were killed by decapitation at one of four time points across the 24-h day (ZT1, ZT6, ZT13, ZT18). Coronal slices (400 μM) containing the NAc and CPu were prepared from each animal with a vibrating tissue slicer while immersed in oxygenated aCSF containing: NaCl (126 mM), KCl (2.5 mM), NaH_2PO_4 (1.2 mM), $CaCl_2$ (2.4 mM), $MgCl_2$ (1.2 mM), $NaHCO_3$ (25 mM), glucose (11 mM), L-ascorbic acid (0.4 mM), and pH was adjusted to 7.4. Once sliced, tissue was transferred to the testing chambers containing bath aCSF (32 °C), which flowed at 1 mL/min. A cylindrical carbon fiber microelectrode (100–200 μM length, 7-μM radius) and a bipolar stimulating electrode were initially placed into the CPu. DA was evoked by a single, rectangular, electrical pulse (750 μA, 4 ms), applied every 5 min. Extracellular DA was monitored at the carbon fiber electrode every 100 ms using FSCV by applying a triangular waveform (−0.4 to +1.2 to −0.4 V vs. Ag/AgCl, 400 V/s). Once the extracellular DA response was stable (i.e., did not exceed 10% variation in peak height for three successive stimulations), the process was repeated at two additional locations by moving the carbon fiber electrode and stimulator first to the core of the NAc and then to the shell of the NAc. Immediately following the completion of each brain region, carbon fiber electrodes were calibrated by recording their response (in electrical current, nA) to a known concentration of DA in aCSF (3 μM). Evoked levels of DA were modeled using Michaelis–Menten kinetics, as a balance between release and uptake. Michaelis–Menten modeling provides parameters that describe the amount of DA released following stimulation (i.e., the peak-height of the signal) and the maximal rate of DA uptake (V_{max}). We followed standard voltammetric modeling procedures by setting the apparent K_m parameter to 160 nM for each animal based on well-established research on the affinity of DA for the DAT (62), and baseline V_{max} values were allowed to vary as the baseline measure of rate of DA uptake. In a separate set of experiments, a quinpirole concentration-response using two concentrations (30 nM and 100 nM) of the drug was applied cumulatively after establishing stable $[DA]_o$ in the CPu. Each concentration was applied until $[DA]_o$ was stable as described above (45 min per concentration), before adding the subsequent concentration. In the acute cocaine experiments, a saturating concentration of cocaine (10 μM) was applied to the slice and $[DA]_o$ was recorded until reaching stability as described above. All voltammetry data were collected and modeled using Demon Voltammetry and Analysis Software (63). All data were compared across groups using either two-way or one-way ANOVA using GraphPad statistical software. When significant main effects were obtained ($P < 0.05$), differences between groups at each dose were tested using either Tukey's Multiple Comparison or Bonferroni post hoc tests.

Western Blot Hybridization. Mice were killed at 1 and 6 h into the light- and dark-phases at ZT1, ZT6, ZT13, and ZT18. Brains were rapidly removed and placed into ice-cold oxygenated aCSF. For precise microdissections of striatal regions, a vibrating tissue slicer was used to prepare 300- to 400-μm-thick slices of brain tissue, from which the NAc and CPu were free-hand dissected. Samples were flash-frozen in isopentane (2-methylbutane; Fisher Scientific) and stored at −80 °C freezer.

Tissues dissected from the NAc and CPu were homogenized in RIPA buffer (150 mM NaCl, 1.0% Triton-X-100, 0.5% Sodium Deoxycholate, 0.1% SDS, 50mM Trizma Base, pH 8.0) and centrifuged at 12,000 × *g* for 30 min. Protein concentration was determined by BCA protein assay kit (ThermoScientific). Because we have previously shown that the levels of TH in DAT knockout mice are reduced 96% compared with WT mice (40), 60 μg of protein from DAT KO mice, and 5 μg of protein from DAT WT mice were used for Western blot analyses. Samples were loaded onto 10% (wt/vol) SDS polyacrylamide gels and transferred onto PVDF membranes (Bio-Rad Laboratories). After incubation with the blocking buffer containing 5% (wt/vol) nonfat milk in Tris-buffered saline, the membranes were probed overnight at 4 °C with mouse antityrosine hydroxylase antibody (Santa Cruz Biotechnology). Following primary antibody incubation, the membranes were incubated with goat anti-mouse antibody conjugated with peroxidase. Western bots were visualized by enhanced chemiluminescence substrate solution (ThermoScientific) and exposure to X-ray film. Films were analyzed densitometrically using ImageJ (NIH). Actin was used as an internal control. The band density was normalized to its respective actin level for quantitation of TH expression.

ACKNOWLEDGMENTS. This work was funded by National Institutes of Health Grants R01 DA021325, R01 DA030161, U01 AA014091, P01 AA021099 (to S.R.J.), P50 DA006634 (to S.R.J., M.J.F., R.A.E., R.C.), K99 DA031791 (to M.J.F.), T32 DA007246 (to M.J.F.) K01 DA025279 (to R.A.E.), and F31 DA035558 (to J.H.R.).

1. Madras BK, Miller GM, Fischman AJ (2005) The dopamine transporter and attention-deficit/hyperactivity disorder. *Biol Psychiatry* 57(11):1397–1409.
2. Mazei-Robison MS, et al. (2008) Anomalous dopamine release associated with a human dopamine transporter coding variant. *J Neurosci* 28(28):7040–7046.
3. Brunswick DJ, Amsterdam JD, Mozley PD, Newberg A (2003) Greater availability of brain dopamine transporters in major depression shown by [99m Tc]TRODAT-1 SPECT imaging. *Am J Psychiatry* 160(10):1836–1841.
4. Newberg A, Amsterdam J, Shults J (2007) Dopamine transporter density may be associated with the depressed affect in healthy subjects. *Nucl Med Commun* 28(1):3–6.
5. Zahniser NR, Sorkin A (2004) Rapid regulation of the dopamine transporter: Role in stimulant addiction? *Neuropharmacology* 47(Suppl 1):80–91.
6. Schmitt KC, Reith MEA (2010) Regulation of the dopamine transporter: Aspects relevant to psychostimulant drugs of abuse. *Ann N Y Acad Sci* 1187(1187):316–340.
7. Gainetdinov RR, Mohn AR, Caron MG (2001) Genetic animal models: Focus on schizophrenia. *Trends Neurosci* 24(9):527–533.
8. Gainetdinov RR, Mohn AR, Bohn LM, Caron MG (2001) Glutamatergic modulation of hyperactivity in mice lacking the dopamine transporter. *Proc Natl Acad Sci USA* 98(20): 11047–11054.
9. Arguello PA, Gogos JA (2006) Modeling madness in mice: One piece at a time. *Neuron* 52(1):179–196.
10. Drury SS, Theall KP, Keats BJB, Scheeringa M (2009) The role of the dopamine transporter (DAT) in the development of PTSD in preschool children. *J Trauma Stress* 22(6):534–539.
11. Maron E, Nutt DJ, Kuikka J, Tiihonen J (2010) Dopamine transporter binding in females with panic disorder may vary with clinical status. *J Psychiatr Res* 44(1):56–59.
12. Gainetdinov RR, Jones SR, Fumagalli F, Wightman RM, Caron MG (1998) Re-evaluation of the role of the dopamine transporter in dopamine system homeostasis. *Brain Res Brain Res Rev* 26(2–3):148–153.
13. Jones SR, Gainetdinov RR, Caron MG (1999) Application of microdialysis and voltammetry to assess dopamine functions in genetically altered mice: Correlation with locomotor activity. *Psychopharmacology (Berl)* 147(1):30–32.
14. Staley JK, Hearn WL, Ruttenber AJ, Wetli CV, Mash DC (1994) High affinity cocaine recognition sites on the dopamine transporter are elevated in fatal cocaine overdose victims. *J Pharmacol Exp Ther* 271(3):1678–1685.
15. Mash DC, Pablo J, Ouyang Q, Hearn WL, Izenwasser S (2002) Dopamine transport function is elevated in cocaine users. *J Neurochem* 81(2):292–300.
16. Paulson PE, Robinson TE (1994) Relationship between circadian changes in spontaneous motor activity and dorsal versus ventral striatal dopamine neurotransmission assessed with on-line microdialysis. *Behav Neurosci* 108(3):624–635.
17. Castañeda TR, de Prado BM, Prieto D, Mora F (2004) Circadian rhythms of dopamine, glutamate and GABA in the striatum and nucleus accumbens of the awake rat: Modulation by light. *J Pineal Res* 36(3):177–185.
18. Léna I, et al. (2005) Variations in extracellular levels of dopamine, noradrenaline, glutamate, and aspartate across the sleep-wake cycle in the medial prefrontal cortex and nucleus accumbens of freely moving rats. *J Neurosci Res* 81(6):891–899.
19. Miller JD, Farber J, Gatz P, Roffwarg H, German DC (1983) Activity of mesencephalic dopamine and non-dopamine neurons across stages of sleep and walking in the rat. *Brain Res* 273(1):133–141.
20. Steinfels GF, Heym J, Strecker RE, Jacobs BL (1983) Behavioral correlates of dopaminergic unit activity in freely moving cats. *Brain Res* 258(2):217–228.
21. Trulson ME, Preussler DW, Howell GA (1981) Activity of substantia nigra units across the sleep-waking cycle in freely moving cats. *Neurosci Lett* 26(2):183–188.
22. Trulson ME, Preussler DW (1984) Dopamine-containing ventral tegmental area neurons in freely moving cats: Activity during the sleep-waking cycle and effects of stress. *Exp Neurol* 83(2):367–377.

23. Trulson ME (1985) Simultaneous recording of substantia nigra neurons and voltammetric release of dopamine in the caudate of behaving cats. *Brain Res Bull* 15(2): 221–223.
24. Dahan L, et al. (2007) Prominent burst firing of dopaminergic neurons in the ventral tegmental area during paradoxical sleep. *Neuropsychopharmacology* 32(6):1232–1241.
25. Hobson JA, McCarley RW, Wyzinski PW (1975) Sleep cycle oscillation: Reciprocal discharge by two brainstem neuronal groups. *Science* 189(4196):55–58.
26. Foote SL, Aston-Jones G, Bloom FE (1980) Impulse activity of locus coeruleus neurons in awake rats and monkeys is a function of sensory stimulation and arousal. *Proc Natl Acad Sci USA* 77(5):3033–3037.
27. Aston-Jones G, Bloom FE (1981) Activity of norepinephrine-containing locus coeruleus neurons in behaving rats anticipates fluctuations in the sleep-waking cycle. *J Neurosci* 1(8):876–886.
28. Trulson ME, Jacobs BL (1975) Raphe neurons: Depression of activity by L-5-hydroxytryptophan. *Brain Res* 97(2):350–355.
29. Puizillout JJ, Gaudin-Chazal G, Daszuta A, Seyfritz N, Ternaux JP (1979) Release of endogenous serotonin from "encéphale isolé" cats. II—Correlations with raphe neuronal activity and sleep and wakefulness. *J Physiol (Paris)* 75(5):531–537.
30. Steininger TL, Alam MN, Gong H, Szymusiak R, McGinty D (1999) Sleep-waking discharge of neurons in the posterior lateral hypothalamus of the albino rat. *Brain Res* 840(1–2):138–147.
31. Terman M, Terman JS (1975) Control of the rat's circadian self-stimulation rhythm by light-dark cycles. *Physiol Behav* 14(6):781–789.
32. Roberts DCS, Andrews MM (1997) Baclofen suppression of cocaine self-administration: Demonstration using a discrete trials procedure. *Psychopharmacology (Berl)* 131(3):271–277.
33. Brebner K, Froestl W, Andrews M, Phelan R, Roberts DCS (1999) The GABA(B) agonist CGP 44532 decreases cocaine self-administration in rats: demonstration using a progressive ratio and a discrete trials procedure. *Neuropharmacology* 38(11):1797–1804.
34. Roberts DCS, Brebner K, Vincler M, Lynch WJ (2002) Patterns of cocaine self-administration in rats produced by various access conditions under a discrete trials procedure. *Drug Alcohol Depend* 67(3):291–299.
35. Pothos EN (2002) Regulation of dopamine quantal size in midbrain and hippocampal neurons. *Behav Brain Res* 130(1-2):203–207.
36. Egaña LA, et al. (2009) Physical and functional interaction between the dopamine transporter and the synaptic vesicle protein synaptogyrin-3. *J Neurosci* 29(14): 4592–4604.
37. Bello EP, et al. (2011) Cocaine supersensitivity and enhanced motivation for reward in mice lacking dopamine D2 autoreceptors. *Nat Neurosci* 14(8):1033–1038.
38. Bianco LE, Unger EL, Earley CJ, Beard JL (2009) Iron deficiency alters the day-night variation in monoamine levels in mice. *Chronobiol Int* 26(3):447–463.
39. Sleipness EP, Sorg BA, Jansen HT (2007) Diurnal differences in dopamine transporter and tyrosine hydroxylase levels in rat brain: Dependence on the suprachiasmatic nucleus. *Brain Res* 1129(1):34–42.
40. Jones SR, et al. (1998) Profound neuronal plasticity in response to inactivation of the dopamine transporter. *Proc Natl Acad Sci USA* 95(7):4029–4034.
41. Sleipness EP, Jansen HT, Schenk JO, Sorg BA (2008) Time-of-day differences in dopamine clearance in the rat medial prefrontal cortex and nucleus accumbens. *Synapse* 62(12):877–885.
42. Wirz-Justice A (1974) Possible circadian and seasonal rhythmicity in an in vitro model: Monoamine uptake in rat brain slices. *Experientia* 30(11):1240–1241.
43. O'Neill RD, Fillenz M (1985) Simultaneous monitoring of dopamine release in rat frontal cortex, nucleus accumbens and striatum: Effect of drugs, circadian changes and correlations with motor activity. *Neuroscience* 16(1):49–55.
44. Sumaya IC, Byers DM, Irwin LN, Del Val S, Moss DE (2004) Circadian-dependent effect of melatonin on dopaminergic D2 antagonist-induced hypokinesia and agonist-induced stereotypies in rats. *Pharmacol Biochem Behav* 78(4):727–733.
45. Andretic R, Hirsh J (2000) Circadian modulation of dopamine receptor responsiveness in *Drosophila melanogaster*. *Proc Natl Acad Sci USA* 97(4):1873–1878.
46. Pendyam S, Mohan A, Kalivas PW, Nair SS (2012) Role of perisynaptic parameters in neurotransmitter homeostasis—Computational study of a general synapse. *Synapse* 66(7):608–621.
47. Cragg SJ (2003) Variable dopamine release probability and short-term plasticity between functional domains of the primate striatum. *J Neurosci* 23(10):4378–4385.
48. Cragg SJ, Hille CJ, Greenfield SA (2000) Dopamine release and uptake dynamics within nonhuman primate striatum in vitro. *J Neurosci* 20(21):8209–8217.
49. Grace AA, Floresco SB, Goto Y, Lodge DJ (2007) Regulation of firing of dopaminergic neurons and control of goal-directed behaviors. *Trends Neurosci* 30(5):220–227.
50. Chiu NT, et al. (2011) Relationship between striatal dopamine transporter availability and sleep quality in healthy adults. *Mol Imaging Biol* 13(6):1267–1271.
51. Kume K, Kume S, Park SK, Hirsh J, Jackson FR (2005) Dopamine is a regulator of arousal in the fruit fly. *J Neurosci* 25(32):7377–7384.
52. Wisor JP, et al. (2001) Dopaminergic role in stimulant-induced wakefulness. *J Neurosci* 21(5):1787–1794.
53. Andersen ML, Sawyer EK, Carroll FI, Howell LL (2012) Influence of chronic dopamine transporter inhibition by RTI-336 on motor behavior, sleep, and hormone levels in rhesus monkeys. *Exp Clin Psychopharmacol* 20(2):77–83.
54. Boutrel B, Koob GF (2004) What keeps us awake: The neuropharmacology of stimulants and wakefulness-promoting medications. *Sleep* 27(6):1181–1194.
55. Earley CJ, et al. (2011) The dopamine transporter is decreased in the striatum of subjects with restless legs syndrome. *Sleep* 34(3):341–347.
56. Earley CJ, et al. (2013) Increased synaptic dopamine in the putamen in restless legs syndrome. *Sleep* 36(1):51–57.
57. Golicki D, Bala MM, Niewada M, Wierzbicka A (2010) Modafinil for narcolepsy: Systematic review and meta-analysis. *Med Sci Monit* 16(8):RA177–RA186.
58. Ramar K, Olson EJ (2013) Management of common sleep disorders. *Am Fam Physician* 88(4):231–238.
59. De la Herrán-Arita AK, García-García F (2013) Current and emerging options for the drug treatment of narcolepsy. *Drugs* 73(16):1771–1781.
60. Sforza E, Jouny C, Ibanez V (2003) Time course of arousal response during periodic leg movements in patients with periodic leg movements and restless legs syndrome. *Clin Neurophysiol* 114(6):1116–1124.
61. Johanson CE, Balster RL, Bonese K (1976) Self-administration of psychomotor stimulant drugs: the effects of unlimited access. *Pharmacol Biochem Behav* 4(1):45–51.
62. Wu Q, Reith MEA, Wightman RM, Kawagoe KT, Garris PA (2001) Determination of release and uptake parameters from electrically evoked dopamine dynamics measured by real-time voltammetry. *J Neurosci Methods* 112(2):119–133.
63. Yorgason JT, España RA, Jones SR (2011) Demon voltammetry and analysis software: analysis of cocaine-induced alterations in dopamine signaling using multiple kinetic measures. *J Neurosci Methods* 202(2):158–164.